Dynamic Leading-edge Stagnation Point Determination Utilizing an Array of Hot-film Sensors with Unknown Calibration

Joel C. Ellsworth[1]
NASA Armstrong Flight Research Center, Edwards, California, 93523

During flight-testing of the National Aeronautics and Space Administration (NASA) Gulfstream III (G-III) airplane (Gulfstream Aerospace Corporation, Savannah, Georgia) SubsoniC Research Aircraft Testbed (SCRAT) between March 2013 and April 2015 it became evident that the sensor array used for stagnation point detection was not functioning as expected. The stagnation point detection system is a self calibrating hot-film array; the calibration was unknown and varied between flights, however, the channel with the lowest power consumption was expected to correspond with the point of least surface shear. While individual channels showed the expected behavior for the hot-film sensors, more often than not the lowest power consumption occurred at a single sensor (despite in-flight maneuvering) in the array located far from the expected stagnation point. An algorithm was developed to process the available system output and determine the stagnation point location. After multiple updates and refinements, the final algorithm was not sensitive to the failure of a single sensor in the array, but adjacent failures beneath the stagnation point crippled the algorithm.

Nomenclature

CFD	=	computational fluid dynamics
G-III	=	Gulfstream III (Gulfstream Aerospace Corporation, Savannah, Georgia)
NASA	=	National Aeronautics and Space Administration
SCRAT	=	SubsoniC Research Aircraft Testbed

I. Overview

In line with the recommendations of the National Research Council,[1] the National Aeronautics and Space Administration (NASA) Armstrong Flight Research Center (AFRC) (Edwards, California) applied their Gulfstream III (G-III) aircraft (Gulfstream Aerospace Corporation, Savannah, Georgia), tail number N804NA (Fig. 1), to serve as a testbed for aeronautics flight research experiments. The aircraft is commonly referred to as the "SCRAT," which stands for "SubsoniC Research Aircraft Testbed".[2] A number of sensors have been added to the SCRAT to collect airworthiness and research data for a variety of flight projects, including: wing pressure measurements, structural accelerometers, control surface positions, aircraft state information, air data parameters, pilot control inputs and forces, a hot film array, a fiber optic sensing system (FOSS), engine parameters, and wing strain measurements. The onboard data collection system also has excess capacity for future expansion. This paper focuses on the hot-film array, which was installed to track the stagnation point location throughout flight for varying flap deflections.

[1] Aerospace Engineer, Aerodynamics and Propulsion Branch, P.O. Box 273 / MS 2228, not an AIAA member.

Figure 1. The NASA G-III SubsoniC Research Aircraft Testbed in flight.

A 36-element Senflex® (Tao of Systems Integration, Inc., Hampton, Virginia) hot-film sensor array[3] was installed on the leading edge surface of the left wing (Fig. 2) and arranged so that the sensors bracket the area within which the stagnation point is expected to be. Each element consists of a narrow metal film on a flexible polyimide substrate. While stronger than a wire of similar size, the metal film is fragile. The element is connected to a constant voltage anemometry bridge to complete the individual sensors of the array. There are eight sensors on the upper surface of the wing and 24 on the lower surface, with a sensor spacing of 0.22 inches. The nature of the hot-film sensor means that power consumption is a function of the local shear stress at the wing surface. As the shear increases, the power consumption increases. As the shear decreases, the power consumption decreases to a minimum when the stagnation point lies over the sensor. By observing the power consumption across the array, the location of the stagnation point should have been easily identified by simply identifying the sensor that was consuming the least power. The electronics box powering the hot-film array also served as a data processing unit for the constant voltage hot-film sensors, and reported values proportional to voltage and current for each sensor. These values are easily converted to power consumption by multiplying them together and dividing by a specified factor. The electronics box also uses the four remaining sensors (one on the upper surface, three on the lower) to measure the local temperature to calibrate the sensor array when it is powered on. This calibration ensures that the sensor array compensates properly for day to day variations in atmospheric temperature and compensates for variations in resistance between the hot film bridges. This setup results in the calibration being different for every flight, with the raw data unavailable and calibration being unknown.

Figure 2. The hot-film array placed on the leading-edge surface of the left wing.

II. Flight-testing

The initial flight-testing of the hot-film array showed that the system could function in flight. In some cases the system functioned well for low-altitude tower flybys, however, the ground level calibration was inadequate for the different conditions experienced at high altitudes, and the system as a whole did not provide useful answers throughout the G-III flight envelope. A comparison of computational fluid dynamics (CFD) predictions for stagnation point and system results from the same flight at multiple flight conditions is presented in Fig. 3. In the figure, blue dots are the system results; the red line represents the CFD prediction.

A representative time history of power consumption through a dynamic maneuver is presented in Fig. 4. The power consumptions have been filtered to reduce noise, but are otherwise unaltered. If the system had functioned as was desired, the channel with the lowest power consumption should have changed as the aircraft changed angle of attack (alpha). Instead, power clearly altered with changes in alpha but the sensor consuming the least power remained the same, indicating that the system responded to changes in angle of attack but not in the desired fashion.

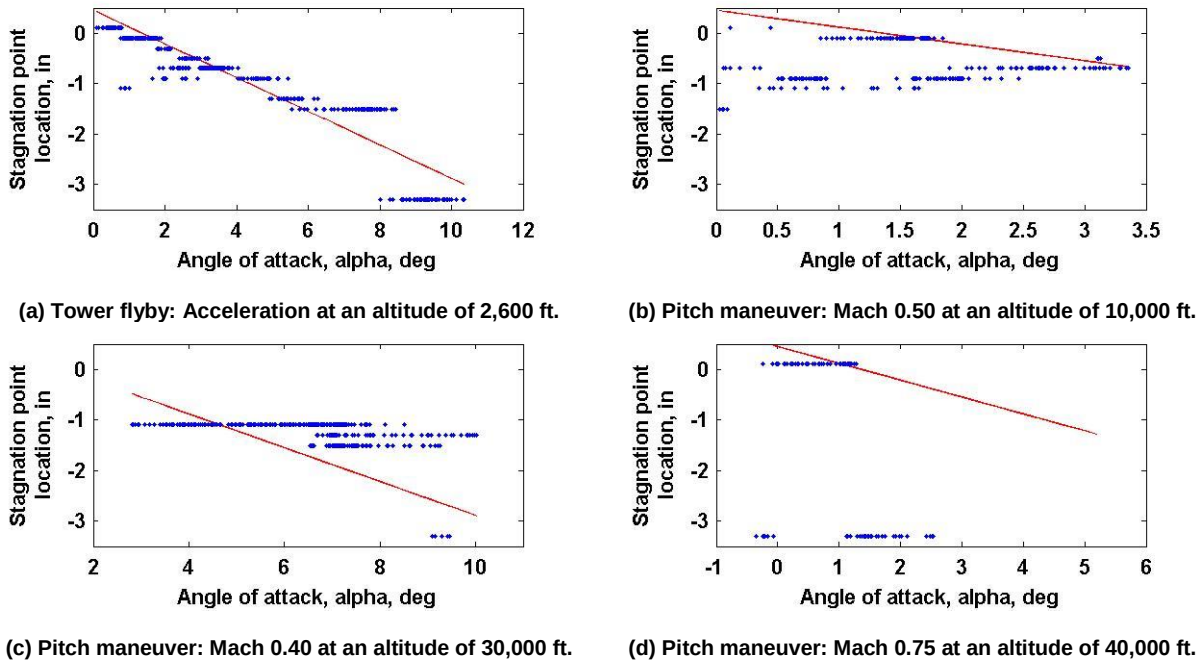

Figure 3. Full system results from the same flight for four representative flight maneuvers with varying angle of attack at differing flight conditions.

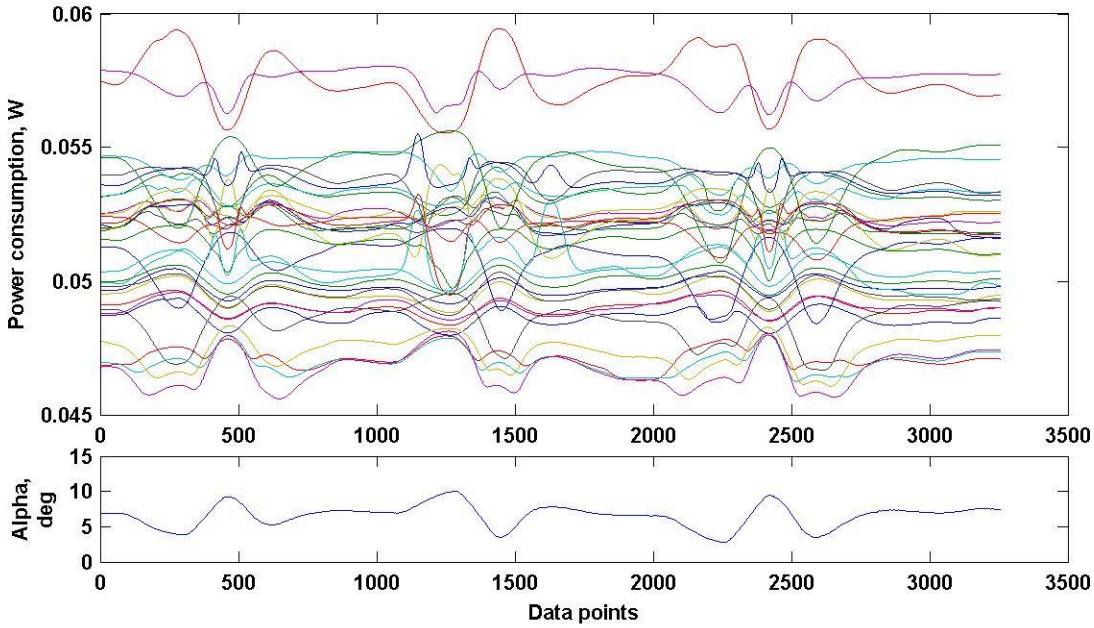

Figure 4. Power consumption for a pitch maneuver, representative of the flight-test results.

III. Algorithm Development

The initial approach to extracting useful data was to identify a calibration that would remove the signal biases and normalize the slopes to a common value. Ideally, this approach would restore the desired functionality of the system. A genetic algorithm was developed to find calibrations based purely on flight data because there were no wind-tunnel data available for this sensor system. Unfortunately, the changing (and unknowable) calibrations prevented a good solution from being found. Individually, the sensors behaved as would be expected, with power consumption varying with angle of attack; therefore, a post-flight analysis algorithm was developed to look for a signature pattern of a decrease in power followed by an increase on a single sensor over time. This occurrence could indicate that the stagnation point had just crossed a sensor. If the pattern repeated across neighboring sensors with the time of minimum signal value shifting in time, there would be a strong probability that the stagnation point were moving across those sensors. Accordingly, an algorithm was developed to find the edge boundary between two neighboring sensors where one was showing increasing power consumption and its neighbor showing decreasing power consumption. These two sensors would be expected to be the closest sensors to the stagnation point. As the location of the stagnation point moved in time, due to maneuvering, the tracked pattern would form what is referred to as the "edge path."

This initial algorithm worked well for some flight-test maneuvers, but not for others. The problem was that multiple locations showed the pattern of increasing and decreasing power consumption, so the algorithm was modified to compare the duration of the edge paths and select the longest one as the most likely stagnation point location. The algorithm was later further modified to re-initialize the search, because the signal was lost when the aircraft was flying at a steady angle of attack, such as between pitch maneuvers. The resulting algorithm followed the stagnation point through 80-90% of the dynamic pitching maneuvers. The plot format made it relatively easy to spot the locations where the algorithm did not properly follow the edge path.

The largest deficiency of the modified algorithm was its reliance on a moving stagnation point. When the stagnation point stops moving, the edge boundary is lost in noise, and the algorithm, not knowing to not move the stagnation point, only looks for increasing or decreasing values. Figures 5 and 6, respectively, demonstrate successful and unsuccessful searches for the stagnation point. The figures are broken into three separate charts. The upper chart shows increasing (red) and decreasing (blue) power consumption values. The magenta lines are potential edge matches, and the green lines are the raw and filtered "best" match. The middle chart shows angles of attack (and aileron deflection in Fig. 6) and is provided for reference. The lower chart shows the probable stagnation point in blue circles, a filtered version as green dots, and where the stagnation point is predicted to be from CFD results for a wing with zero flap deflection as a red line. The stagnation point location is given in inches from the leading edge, measured along the surface, with negative values representing the lower wing surface. Figure 5 shows that the algorithm generally puts the stagnation point close to the CFD solution. The region that is in error is easy to spot, as is the correct stagnation point. Figure 6 shows the algorithm failing to find the signal in a yaw roll maneuver with minimal change in angle of attack. Because the angle of attack only varies by a very small amount, the algorithm gets lost, and restarts repeatedly. The algorithm does frequently find the stagnation point, but its output is not reliable.

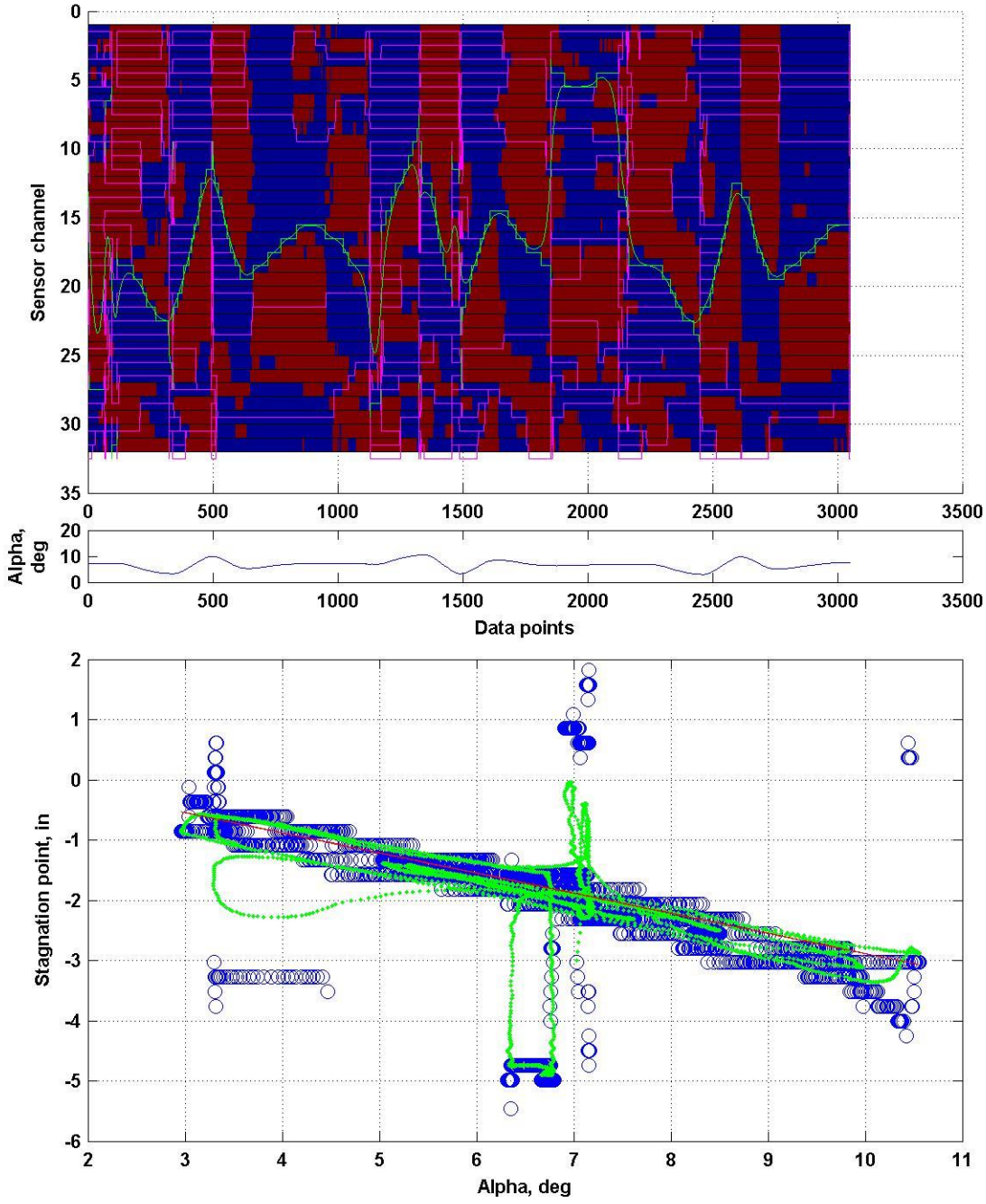

Figure 5. Algorithm performance in a pitch maneuver at Mach 0.35 and an altitude of 20,000 ft.

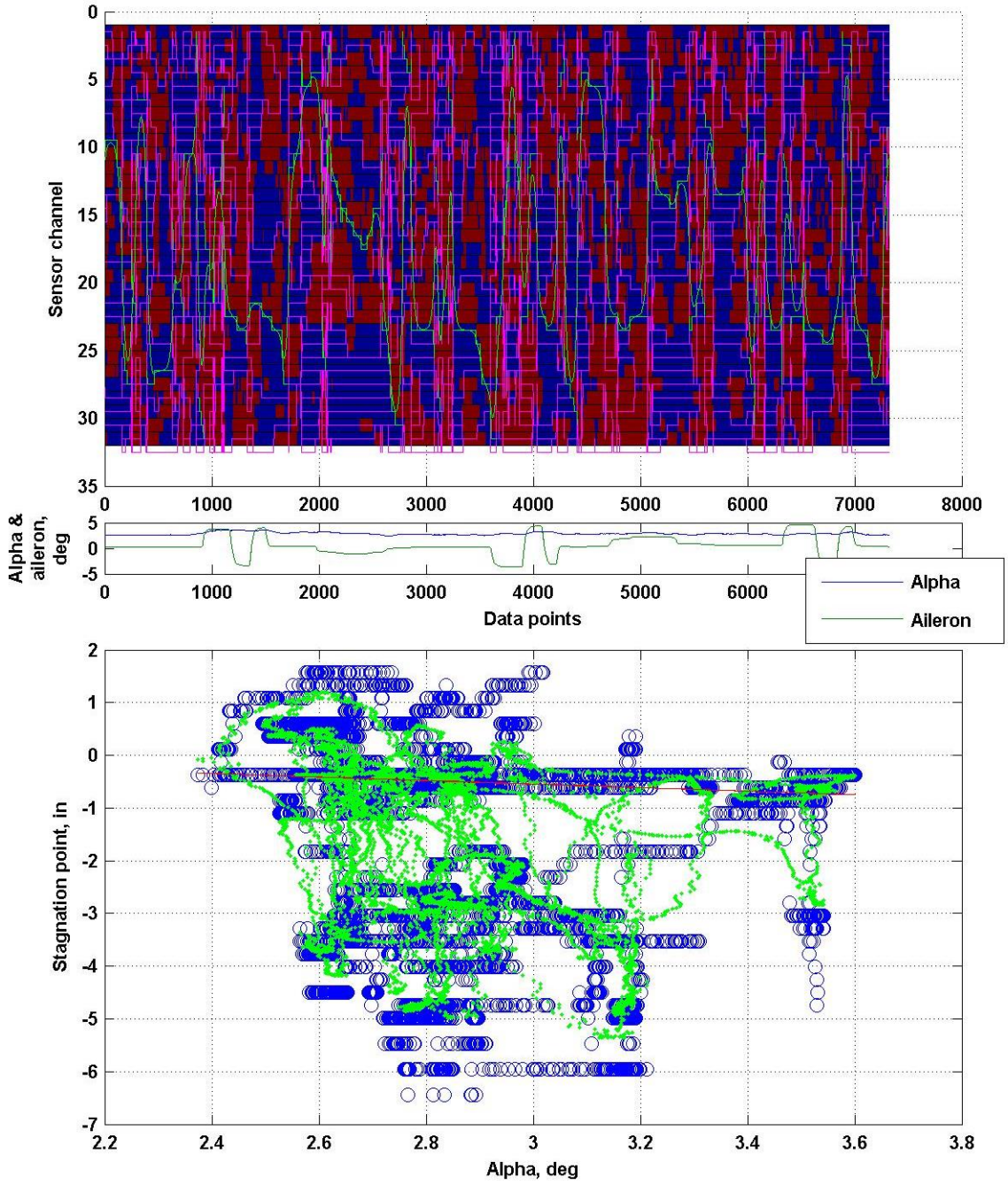

Figure 6. Algorithm performance in a yaw-roll maneuver at Mach 0.5 and an altitude of 20,000 ft.

As flights progressed, several data channels on the upper surface and near the leading edge became non-functional due to small fractures in the wiring traces. Initially these fractures were assumed not to be problematic, as the algorithm could handle a single channel with a constant value. In addition to multiple neighboring channels eventually being lost, however, the signals still recorded low-amplitude noise, which only served to confuse the algorithm and pull the solution away from the correct solution. Figure 7 shows a comparison of algorithm performance for a pitch maneuver from two different flights with all channels functioning and three channels failed.

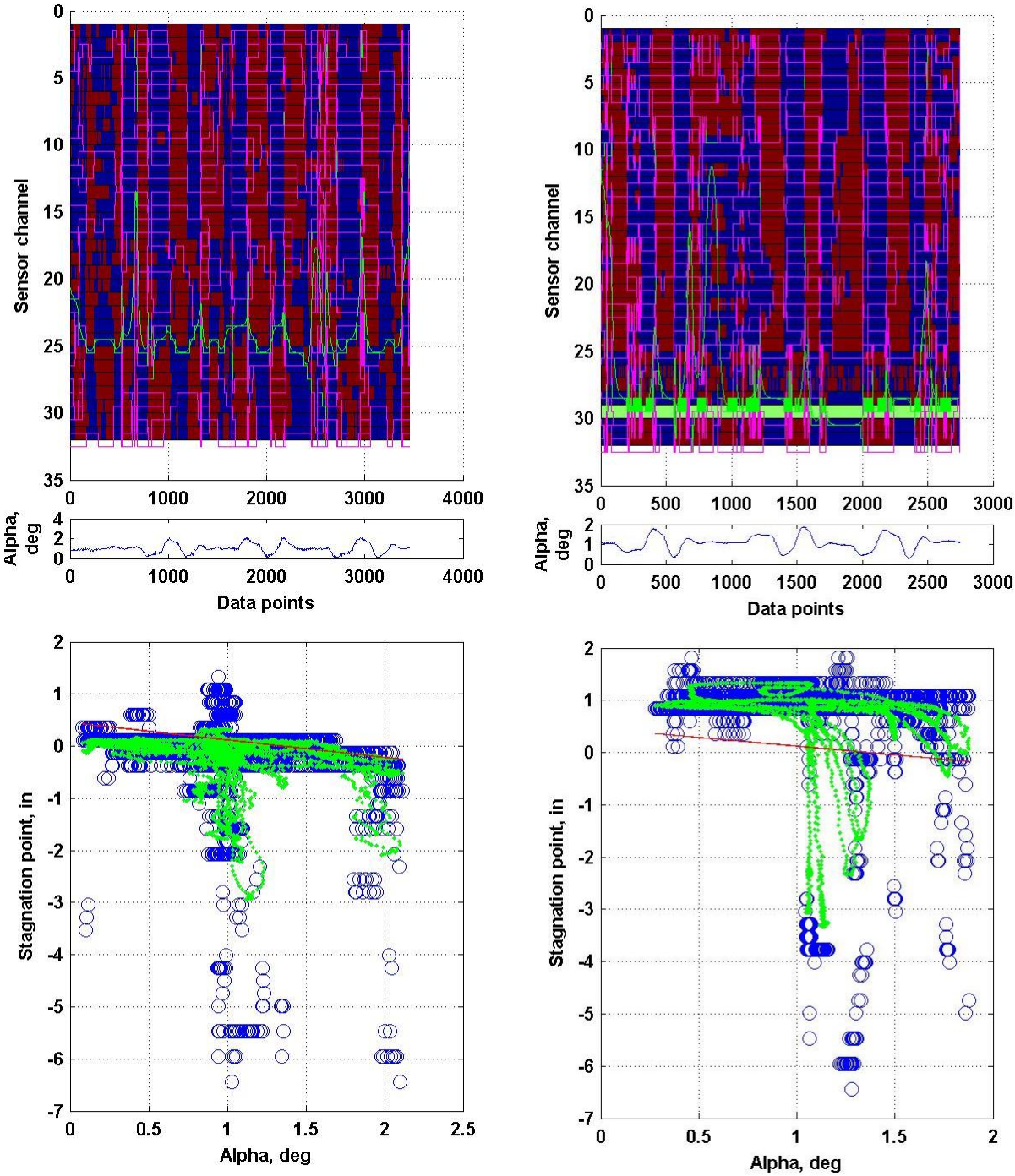

(a) All channels functioning.

(b) Channels 26, 27, and 29 failed.

Figure 7. Comparison of algorithm performance for a pitch maneuver from two different flights, with all channels functioning and three channels failed for a pitch maneuver at Mach 0.7 and an altitude of 20,000 ft.

As a consequence of the problems seen in Fig. 7(b) the algorithm was modified to ignore the failed signals. The tracking portion of the algorithm itself was not altered, but the input was altered so that the failed channels were removed and the functional channels became neighbors in the analyzed data. This change increased the area represented by each sensor, decreasing the accuracy of the stagnation point location for those sensors neighboring a

failed sensor. The same flight data shown in Fig. 7(b) were reprocessed with the updated algorithm to yield the useable result shown in Fig. 8, extending the usefulness of the algorithm to analyze a few more flights. The increasing number of sensor failures combined with flight condition, however, resulted in the stagnation point falling on failed sensors. By the time the flight campaign was finished, sensor channels 23, 26, 27, 28, 29, 30, and 32 had failed, yielding insufficient data to determine the stagnation point. The charts in Fig. 9 show the algorithm attempting to find the stagnation point as it falls upon failed sensors.

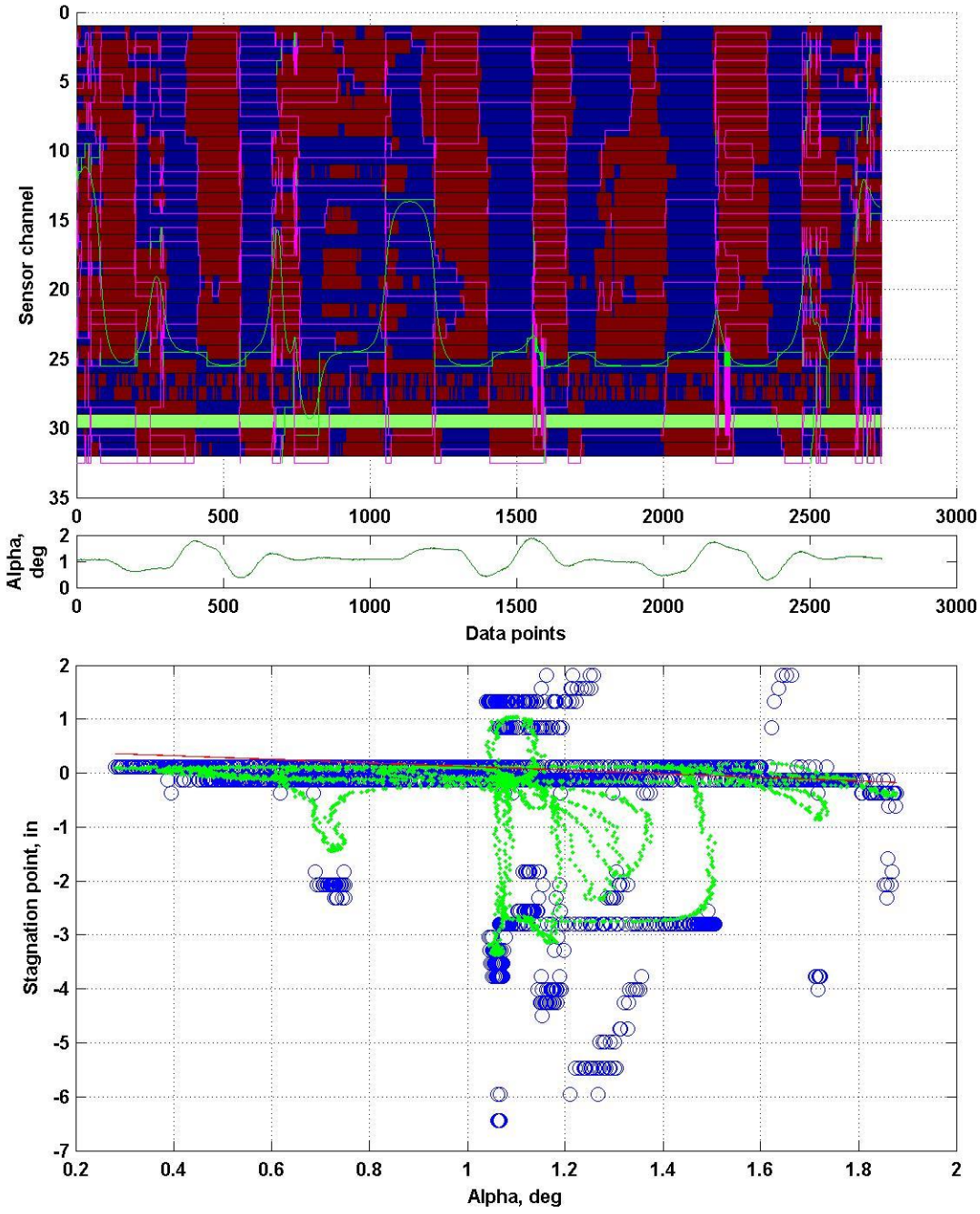

Figure 8. Results from the updated algorithm, tolerant to failed channels; the same data as presented in figure 7(b) (Mach 0.7 and an altitude of 20,000 ft).

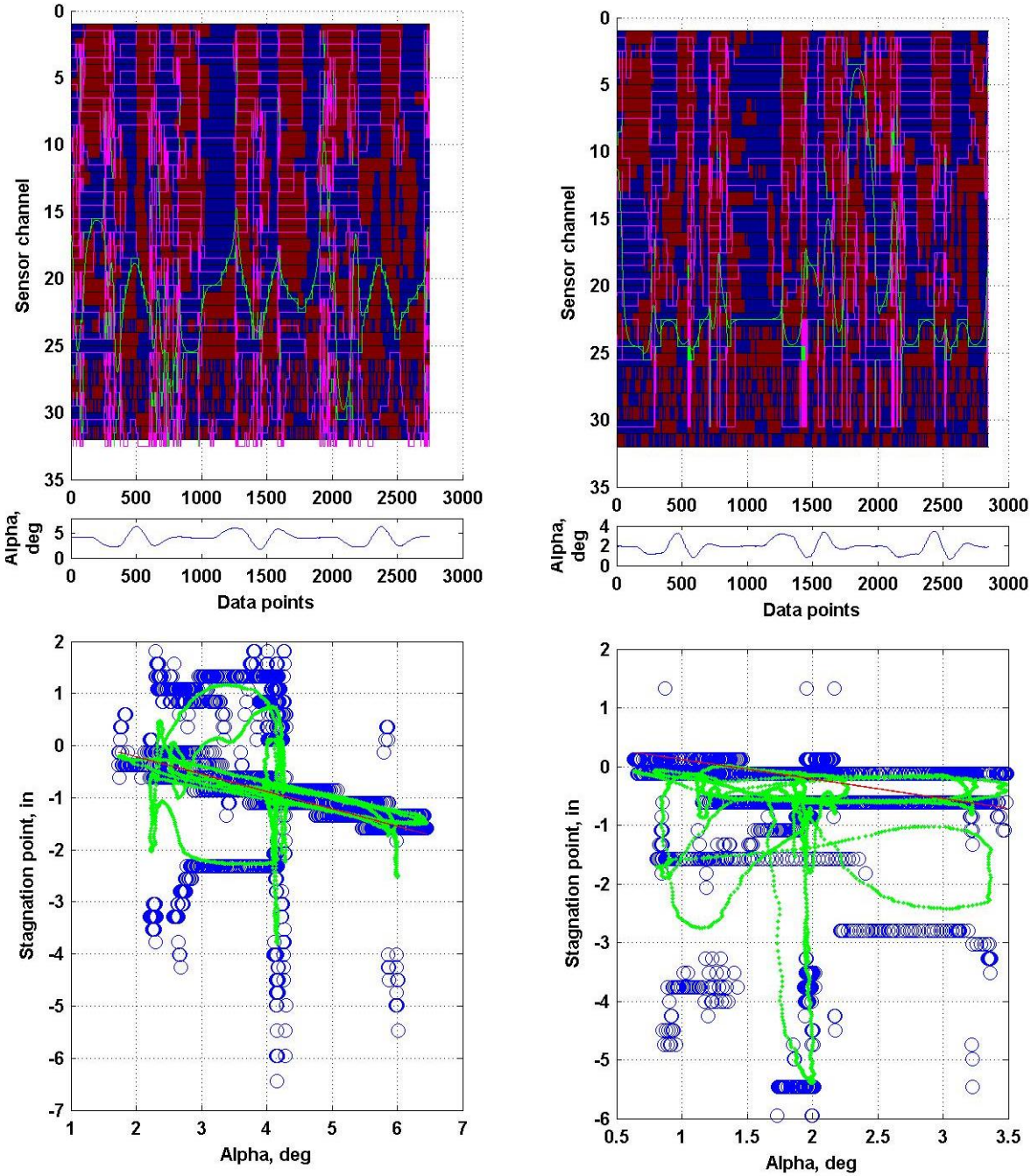

(a) Results at Mach 0.45 at an altitude of 20,000 ft.

(b) Results at Mach 0.6 and an altitude of 20,000 ft.

Figure 9. Algorithm performance for different flight conditions on the same flight; stagnation point over functional sensors (a), and non-functional sensors (b).

IV. Conclusion

An algorithm was developed to extract useful test data from a hot-film array mounted on the leading edge of the left wing of a Gulfstream G-III airplane (Gulfstream Aerospace Corporation, Savannah, Georgia), because the existing algorithm was not performing as expected during flight-testing. The basic operational principles of a hot-film sensor were used to develop an algorithm that did not require calibration of the individual hot-film sensors. As the flight-test series progressed, the algorithm was modified several times to be better able to handle changing conditions and failed sensor channels. Eventually, as adjacent sensors failed, the algorithm was rendered useless as the increased airspeeds moved the stagnation point over the failed sensors. As long as the stagnation point was above the functioning hot-film sensors, the algorithm was able to track the stagnation point through dynamic pitching maneuvers with a high degree of reliability

References

[1]National Research Council of the National Academies, *Recapturing NASA's Aeronautics Flight Research Capabilities*, The National Academies Press, Washington, D. C., 2012.

[2]Baumann, E., Hernandez, J., and Ruhf, J., "An Overview of NASA's SubsoniC Research Aircraft Testbed (SCRAT)," AIAA-2013-5083, 2013.

[3]Tao Systems, Senflex® Multi-Element Surface Hot-Film Sensors, http://www.taosystem.com/products/senflex/ [cited 22 November 2016].